

Supplementary Online Materials

Definitions

This manuscript refers to a number of different types of mouse models. For clarity, the terms for these models have been defined below.

Genetically Engineered Mouse (GEM) – Model based on manipulation of the mouse genome, either through transgenic incorporation of exogenous DNA elements or following homologous recombination in embryonic stem cells.

transplantation model – refers to all mouse models in which tumor cells or tumor fragments are transplanted into a mouse. Unless otherwise indicated, syngeneic autografts were used as examples of transplantation models.

xenograft – refers to models in which human tumor cells or tumor fragments are transplanted into immunodeficient mice.

syngeneic autograft – refers to models in which murine tumor cells or tumor fragments are transplanted into histocompatible, immune-competent mice.

ectopic – term that describes the site of transplantation as being different than that from which the transplanted material was derived.

subcutaneous (SC) – describes the location of an ectopic transplant as being under the skin.

orthotopic – term that describes the site of transplantation as being analogous to that from which the transplanted material was derived, in this case the pancreas.

responder – used to describe tumors in a drug treatment study that were observed to have decreased in volume at any point.

Statistical Analyses

Statistical analyses were carried out using GraphPad Prism version 5.00 for Windows, GraphPad Software, San Diego California USA. Distinction of responders by Cleaved Caspase 3 was determined using Extreme Studentized Deviate outlier analysis. Significance of metastasis data was determined by Fischer's Exact test. Significance of endothelial proliferation data was determined by Student's T test due to small sample

size. All other comparisons were made using Mann-Whitney U test. Box plots show range, median and quartiles.

Animal Use

All studies were conducted in compliance with the institutional and national guidelines of their respective locations.

Cell Lines

The human pancreatic cancer cell line AsPc1 was acquired from ATCC (CRL-1682) and cultured according to instructions. Mouse pancreatic cancer cell lines K8484, K8675 and DT8082 were isolated from tumors arising in KPC mice using a modification of the protocol described by Schreiber et. al, 2004 (1). Briefly, a 3mm³ fragment of PDA was excised, washed in 10mL of cold PBS, and then finely diced with sterile razors. Cells were incubated in 10mL of collagenase solution at 37°C for 30-45 minutes with mixing (1mg/mL collagenase V in DMEM/F12). Cells were spun (100rpm, 5 min.) and resuspended in 0.05% Trypsin/EDTA for 5 min. at 37°C, and then quenched with DMEM supplemented with 10% fetal calf serum and 96µM CaCl₂. Cells were washed 3 times with DMEM/F12 medium and plated in a 6-well Biocoat dish (Becton Dickenson) in the ductal cell medium described previously (1). After 3-4 passages, cells were transferred to standard plastic tissue culture dishes and grown in DMEM + 10% FCS.

Subcutaneous and Orthotopic Tumor Models

1x10⁶ cells suspended in 100µL of PBS were injected subcutaneously into the flanks of nude mice (xenografts) or into immunocompetent mice (syngeneic). For syngeneic

models, recipient mice were descended from mice used to generate the KPC PDA cell lines. Orthotopic tumors with MiaPaca2 were generated as previously described(2). Long (L) and short (S) axes of each tumor were measured with calipers (for subcutaneous tumors) or ultrasound (for orthotopic tumors). Tumor volume (V) was calculated: $V = (L \times S^2)/2$. Tumor volumes were normalized relative to the volume at the start of drug treatment for subcutaneous tumors. Orthotopic tumors were measured on days 7 and 20 following injection of cells and gemcitabine treatment was initiated on day 8. Tumor images were acquired using a pediatric ultrasound machine. This machine was not equipped for 3D reconstruction, so the same formula $V = (L \times S^2)/2$ was used to estimate the tumor volumes and changes. Mice were treated with gemcitabine by intraperitoneal injection on a Q3Dx4 schedule. When appropriate, a fifth dose was given on the final day four hours prior to necropsy for pharmacological analyses.

KPC Mice

KPC mice harbor heterozygous conditional mutant alleles of *Kras* and *p53* as well as a pancreatic-specific Cre recombinase, *Pdx1-Cre*. Mice bearing the *Kras*, *p53* and *Cre* alleles develop a full spectrum of premalignant neoplasms that stochastically undergo loss of the remaining wild-type *Trp53* allele and culminate in overt invasive and metastatic PDA with a mean survival of 4.5 months. The KPC mice utilized in this paper harbor one of two conditional point-mutant *p53* alleles: *p53*^{LSL-R172H} or *p53*^{LSL-R270H} (3). These two mutations have been reported to have largely similar functions in cells and in mice (3). *Kras*^{LSL-G12D/+}, *p53*^{R172H/+}, *Pdx1-Cre* mice have been described (4), but compound mutant mice with the latter allele, *Kras*^{LSL-G12D/+}, *Trp53*^{LSL-R270H/+}, *Pdx1-Cre*,

have not been previously reported. These mice develop advanced pancreatic ductal adenocarcinoma that appears similar to mice harboring the Trp53^{R172H} allele.

Drug Preparation

Gemzar™ (Eli Lilly) powder (a ~48% preparation of difluoro-deoxycytidine, dFdC) was purchased (Hannas, Delaware) and resuspended in sterile normal saline at 5mg/mL dFdC. Additional Gemzar solution was provided by Addenbrooke's Hospital Pharmacy in Cambridge, UK and diluted with normal saline to 5mg/mL dFdC. Drug was administered by intraperitoneal injections at the indicated dose.

IPI-926 was provided by Infinity Pharmaceuticals. IPI-926 was dissolved in a 5% aqueous solution of hydroxypropyl- β -cyclodextran (HPBCD) to a concentration of 5 mg/mL (accounting for batch potency), with sonication and vortexing, and then sterile filtered through a 0.22 μ M Millex GV syringe filter. Working solution was stored at 4°C for up to one week.

Drug Study Treatment Groups

For Figs. 1-3, mice were treated with either saline (20 μ L/g of 0.85% NaCl) or 50-100mg/kg of gemcitabine dissolved in saline. For Fig. 4, the following four treatment groups were described at various timepoints: vehicles- 20 μ L/g 0.85% NaCl + 8 μ L/g 5% HPBCD; gemcitabine- 100mg/kg gemcitabine + 8 μ L/g 5% HPBCD; IPI926- 40mg/kg IPI926 + 20 μ L/g 0.85% NaCl; IPI926/gem- 40mg/kg IPI926 + 100mg/kg gemcitabine.

Survival Study Structure

Enrollment of KPC mice was based on tumor size, measured by ultrasound. For the purpose of enrollment, tumors were scanned in an axial orientation and the long and short axes of the tumor were averaged to give a mean diameter. Mice with mean tumor diameters of 5-10mm were enrolled. For the purpose of measuring tumor growth, tumor volume was quantified by 3D ultrasonography twice weekly until endpoint criteria were met. Endpoint criteria included the development of abdominal ascites, severe cachexia, significant weight loss exceeding 20% of initial weight, or extreme weakness or inactivity. Upon meeting endpoint criteria, when appropriate, mice were administered a final dose of IPI-926 (or vehicle) 6 hours prior to euthanasia and a final dose of gemcitabine (or vehicle) 4 hours prior to euthanasia.

Imaging and Quantification of KPC Pancreatic Tumors

High resolution ultrasound (US) imaging of normal and diseased mouse pancreas using the Vevo 770 System with a 35MHz RMV scanhead (Visual Sonics, Inc.) was performed as described (5). 3D images were produced using the 3D motor arm to collect serial images at 0.25mm intervals through the entire thickness of the tumor. Tumors were outlined on each 2D image and reconstructed to quantify the 3D volume using the integrated Vevo 770 software package.

Contrast Ultrasound

Mice were imaged by ultrasound as described previously (5). Baseline images were acquired in Contrast Mode and then an 80 μ L bolus of unconjugated Vivo Micromarker suspension (VisualSonics, Inc.) was administered via tail vein catheter during acquisition

of a second contrast video. The baseline image was subtracted from the contrast image and the difference was displayed with a contrast setting of 80 and a threshold setting of 0.

MRI

Magnetic resonance imaging experiments were carried out on a Varian MRI system (Varian, Inc, Palo Alto, CA, USA) equipped with a 9.4T horizontal bore cryo-cooled superconducting magnet of 210mm bore and a gradient set of strength 40 G/cm, 120 μ sec risetime and internal diameter 120mm. The imaging probe used was a Varian Millipede of 40mm internal diameter. Mice were anaesthetized with Hypnorm/Hypnovel. Anatomical images were obtained using coronal T2-weighted fast spin-echo (repetition time TR=2000ms, effective echo time TE=25ms, echo train length 8 echoes, 512x512 points, field of view 80x80mm, slice thickness/gap 1.5/0.5mm, 12-15 slices) with chemical shift-selective fat suppression and respiratory gating. All other images were matched to the slice positions and field of view of the anatomical images. Baseline T1 maps were obtained from either T1-weighted RF-spoiled gradient echo imaging (TE=1.52ms, TR=0.05/0.1/0.2/0.5/1/2/5 seconds, 128x128 points, $\alpha = 60^\circ$) or inversion recovery turbo-FLASH (TE=1.52ms, TR=3ms, inversion time TI=0.2/0.5/1/2/5/10 seconds, 128x128 points) using a non-slice-selective hyperbolic secant adiabatic inversion pulse. The dynamic contrast-enhanced (DCE-MRI) time course was acquired using T1-weighted RF-spoiled gradient echo (TE=1.52ms, TR=50ms, 128x128 points, $\alpha = 45^\circ$); 5 time points were acquired before injection of 0.1mmol/kg Gd-DTPA (Magnevist, Bayer Schering Pharma AG) and 100 after, giving a total imaging time of 10 minutes. Additionally, high-resolution (256x256 points) T1-weighted images were acquired before

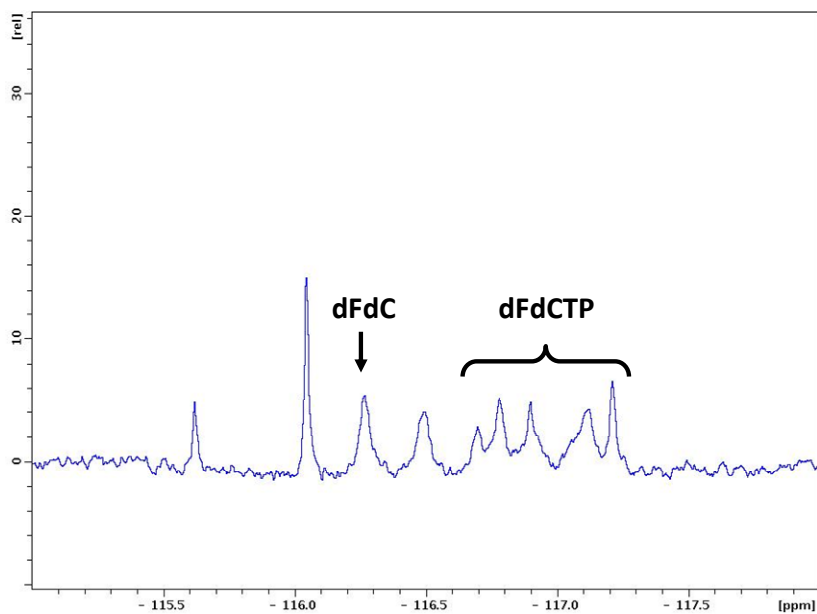
contrast administration and after the DCE-MRI time course, and flip angle mapping data acquired to correct for coil radiofrequency inhomogeneity (6). DCE-MRI data were analyzed in software custom-written in MATLAB 7.4 (The Mathworks, Inc, Natick, MA, USA) using the model of Tofts and Kermode (7, 8) to evaluate the pharmacokinetic parameters K_{trans} and v_e , and additionally calculating the area under the [gadolinium]-time curve over the first 60 seconds post-injection (IAUGC60), as recommended by a panel of experts for vascular-related studies in oncology (9).

¹⁹Fluorine Nuclear Magnetic Resonance

Due to the limited sensitivity of HPLC for detecting dFdCTP in solid tissue, we developed a ¹⁹F-NMR protocol to detect gemcitabine and its metabolites. Mice were treated with indicated drug regimens for 10 days. On the final day, mice from all cohorts were administered an i.p. injection of 100mg/kg gemcitabine and sacrificed after 1 hour. Tissues were rapidly dissected and snap frozen in liquid nitrogen. Tissue specimens were maintained at -80°C until subjected to nucleotide extraction. Samples were homogenized in a Qiagen TissueLyser with a 5mm ball bearing for 2 x 6 minutes at 25KHz, in the presence of 4 volumes of ice-cold acetonitrile (μL acetonitrile = 4 x μg of tissue). An equal volume of water was added and then the sample was spun at 14,000rpm for 10 minutes at 4°C. Supernatant was freeze dried, resuspended in 600 μL of D₂O and transferred to a 5mm standard NMR tube (Wilmad) for ¹⁹F NMR analysis on a Bruker 600 MHz (14.1T) Avance NMR spectrometer using a QNP probe. Acquisition parameters included a 1D pulse sequence of ¹⁹F observation and inverse-gated ¹H decoupling, spectral sweep width of 177 ppm (100000Hz), 4096 scans and 1.65sec of repetition time. Total acquisition time for each sample was about 1 hr 55 min. Trichloro-

fluoro-methane was used for ^{19}F NMR chemical shift calibrations. A broad hump observed in the baseline of ^{19}F NMR spectra was removed by application of Linear-prediction (LP) back projection to the time domain data by using 2000 (number of LP) coefficients and 128 back-prediction points prior to Fourier transformation and phase correction.

A typical fluorine spectrum from a gemcitabine-treated spleen is presented below. No fluorine peaks were observed in untreated tissues. The indicated peaks were identified by adding purified dFdC or dFdCTP to extracted tissue samples. In order to measure the total delivery of gemcitabine to tissue (independent of differences in cellular metabolism between samples), we integrated all observed fluorine peaks using the Bruker Topspin software processing package, providing a measure of total gemcitabine metabolite concentration in the sample. These integrated values were normalized to the tissue weights and presented in arbitrary units. In pilot experiments, we found that six hours after gemcitabine administration, all ^{19}F signals were absent from PDA and control tissues.



IPI926 Pharmacology

IPI926 is a semisynthetic cycloamine derivative (fig. S10). KPC mice harboring pancreatic tumors were treated with 40mg/kg of IPI926 by oral gavage, either singly, once daily for four days or as part of a survival study. In addition, mice received twice weekly injections of either 100mg/kg gemcitabine or 20 μ L/g saline, as indicated. Six hours following the final dose, tissue samples were harvested, snap frozen in liquid nitrogen and stored at -80°C. Mice with abdominal ascites were excluded from analysis. Samples were analyzed by LC/MS, as described below.

Standards and Other Materials for Bioanalytical Methods

Calibration standard stock solutions were prepared by dissolving IPI-926 at a concentration of 2.5 mg/mL in DMSO. Internal standard stock solution was prepared by dissolving IPI-484 (deuterated IPI-926) in DMSO for a final concentration of 2.5 mg/mL. Stock solutions were stored in aliquots at -80°C until further use.

Water (HPLC grade) was obtained from Mallinckrodt Chemicals (Phillipsburg, NJ). Acetonitrile (HPLC grade) was purchased from JT Baker (Phillipsburg, NJ) and formic acid was supplied by Fluka Chemie (Buchs, Switzerland). DMSO was purchased from Sigma (St. Louis, MO). Powdered phosphate buffered saline was reconstituted with water to a 0.1M concentration (pH 7.2)

Sample and Standard Curve Preparation for the Quantitation of IPI-926 in Tumors

Calibration standard and internal standard stock were thawed at room temperature. Internal standard solution was made by diluting IPI-484 into 10% MeOH solution for a final concentration of 25 ng/mL. Calibration curves were prepared in ACN:PBS

homogenization buffer and diluted into internal standard solution. The assay had a final Lower Limit of Quantification (LLOQ) of 0.78 ng/mL. In addition, ACN:PBS with and without internal standard (QC0 and blank, respectively) were included in the analytical run.

Tumor samples were homogenized in 4 volumes of ACN:PBS buffer. Pre-weighed tissue samples were added to 5 mL polycarbonate tubes (SPEX CertiPrep part number 2241-PC) containing a single steel milling ball (SPEX CertiPrep part number 2156) and were homogenized using a Geno/Grinder from SPEX CertiPrep (Metuchen, NJ) for 2 minutes. Homogenates were then filtered using a 0.45 μm low binding hydrophilic multiscreen solvinert plate (Millipore, part number MSRLN0410) and collected in a 96-well receiving plate. The tissue filtrates were then diluted 1:1 (equal volume) and 1/100 into internal standard solution. IPI-926 concentrations for all tissues were preferentially determined using the 1:1 dilution unless any of the replicates for a given tissue required the higher dilution of 1/100 for accurate quantitation.

The IPI-926 concentrations in the samples were determined from the calibration curves generated in homogenization buffer. A dilution factor of 4 was applied to the tissue samples to account for the volume of buffer added to each tissue for homogenization. When adjusting for dilution factor, the assay LLOQ is 3.1 ng/g. No correction for extraction efficiency was applied.

LC-MS/MS Analysis

Sample analysis was performed on an Agilent 1200 from Agilent Technologies (Santa Clara, CA) coupled with an API-4000 mass spectrometer from Applied Biosystems (Foster City, CA) for detection of IPI-926 and Jervine by multiple reaction monitoring (MRM).

Twenty μL of the samples were injected on an analytical column (Symmetry IS, C18, 2.1 x 20 mm, 3.5 μm , from Waters, Milford, MA) and eluted with a 4 minute gradient from 5 – 95% acetonitrile in H_2O , 0.1% (v/v) formic acid.

Mass spectrometric detection of IPI-926, as well as the internal standard IPI-484, was performed by MRM with the following transitions for each compound:

Compound	Q1 mass (m/z)	Q3 mass (m/z)
IPI-926	505.4	114.1
IPI-484	508.3	84.1

The data were acquired and processed using the software Analyst 1.4.1 (Applied Biosystems, Foster City, CA). For the standard curve samples, peak area ratios of analyte (IPI-926) to internal standard (Jervine) were calculated and plotted against the theoretical concentrations. A weighing factor of $1/x^2$ was applied to the data. Sample concentrations, as measured by their peak area ratios (analyte divided by internal standard), were determined from the calibration curves.

Determination of dFdCTP concentration by HPLC

Mice were injected i.p. with 50 or 100mg/kg gemcitabine and sacrificed after four hours. Tissues were rapidly dissected and snap frozen in liquid nitrogen. Specimens were maintained at -80°C until nucleotide extraction. Specimens were ground under liquid nitrogen with a mortar and pestle. The powdered contents were suspended in 0.4N perchloric acid and sonicated in an ice bath. Solids were removed by centrifugation, the pellet was washed with perchloric acid, and the supernatants were combined. Following neutralization with KOH and removal of KClO_4 by centrifugation, a portion of the supernatant was analyzed by high-pressure liquid chromatography, as described (10). The amount of gemcitabine triphosphate was normalized to the ATP level determined in the same sample analysis. Samples with inadequate concentrations of ATP were excluded from analysis.

Immunohistochemistry

Tissues were fixed in 10% formalin solution for 24 hours and transferred to 70% ethanol. Tissues were paraffin embedded, sectioned and rehydrated. For CD31 IHC, sections were unmasked in 10mM EDTA, pH 8.0 in a pressure cooker. For all other antibodies, sections were unmasked in 10mM citric acid, pH 6.0 in a pressure cooker. Endogenous peroxidases were quenched in 3% H_2O_2 /PBS for 20 minutes. Remaining steps were carried out with Vectastain ABC kits appropriate to the species of primary antibody (Vector Labs, Burlingame, CA) with the following modification: blocking serum was supplemented with Protein Blocking Agent (Immunotech/BeckmanCoulter, Fullerton, CA) diluted 1:50. Antigens were developed with DAB Peroxidase Substrate (Vector Labs). The following antibody dilutions were used: Phospho-Histone H3, 1:100 (#9701, Cell

Signaling Technology); Cleaved Caspase 3, 1:100 (#9661, Cell Signaling Technology); CD31, 1:75 (SC-1506). Slides were counterstained with hematoxylin.

Phospho-Histone H3 (PH3) Proliferation Analysis

Tissues were harvested four hours following the last gemcitabine (or vehicle) treatment. For quantification, the number of PH3 positive cells was counted per 40x field. PH3 positive cells were defined as those having positively staining condensed chromatin. For the Smo inhibitor studies, 5 fields per tumor were quantified. For the gemcitabine studies, in most cases at least 6 fields were quantified. However, for a few small tumors, not enough tissue was available and therefore only 3 fields were assessed.

Cleaved Caspase 3 (CC3) Apoptosis Analysis

For gemcitabine study (Figures 1-3), tissues were harvested four hours following the last gemcitabine (or vehicle) treatment. For the Smo inhibitor studies, tissues were harvested either one hour or four hours after the last dose of gemcitabine (or vehicle). This difference in timing did not affect the level of apoptosis within the tumors, suggesting that the increased apoptosis observed in IPI-926/gem treated tumors was the result of the long-term effects of treatment (there was no difference in the amount of apoptosis in KPC tumors treated with vehicle or gemcitabine only). For the Smo inhibitor studies, 5 fields per tumor were quantified. For the gemcitabine studies, in most cases at least 6 fields were quantified. However, in a few cases not enough tissue was available for analysis and therefore only 3 fields were assessed. In tumors with apparent necrosis, necrotic tissues typically took up stain from the CC3 IHC. This necrosis-associated staining was not counted in the CC3 quantification, including cells immediately adjacent to the necrosis. Likewise, cells undergoing anoikis that are positive for CC3 are typically

observed in the lumens of ductal structures formed by well-differentiated neoplastic pancreatic cancer cells. These cells were also excluded from analysis.

Mean Vascular Density and Vascular-Tumor Distance

Tissue sections were probed with anti-CD31 antibodies and counterstained with hematoxylin. Mean vascular density (MVD) was determined as the number of CD31 positive blood vessels per 40X field. In most cases, five fields were quantified per tumor. However, for smaller tumors, only four fields were quantified. The distance separating intratumoral blood vessels and neoplastic cells was determined for twenty randomly chosen blood vessels per tumor. Each intratumoral blood vessels was photographed at 1000X magnification, and the distance to the four nearest tumor cells was measured and the results averaged.

Computer Aided Image Analysis of Mean Vessel Density in Human Tissues

Frozen sections (10 um thickness) were prepared from histologically confirmed samples of infiltrating pancreatic ductal adenocarcinoma or chronic pancreatitis from resection specimens and fixed in 4% paraformaldehyde for 10 minutes at 4°C. Sections were then washed in 1X TBS three times followed by incubation with blocking serum (1X TBS/5% BSA/0.04% Triton X100) for 3 hours at 4°C. Slides were washed with 1X TBS, then incubated overnight at 4°C with primary antibodies diluted in blocking serum (1:200 dilution phycoerythrin labeled mouse anti-CD31 (#340297), Becton Dickonson Systems and 1:100 dilution rabbit anti-TEM8 (H-140), Santa Cruz Biotechnology). After washing in 1XTBS, sections were incubated with 4',6-diamidino-2-phenylindole, dihydrochloride

(DAPI). Slides were coverslipped and labeling visualized using a Nikon E800 microscope.

Immunolabeled slides were scanned at 20x, and up to five 1500x1500 pixel or 735 μm^2 fields located both centrally and at the periphery of the pancreas were extracted and analyzed by color deconvolution (ImageJ software, <http://rsbweb.nih.gov/ij/>). Thresholding was used to convert the image to a binary format in which lighter background staining was eliminated and the remaining areas of staining were converted into particles, which could be individually analyzed by the software. Accounting for variations in staining intensities among slides, exclusion of background staining was based on the average intensity of the overall staining. Any particles measuring less than 150 pixels (73.5 μm^2) were excluded to reduce the degree of large vessel fragmentation and the presence of single immunoreactive cells. To determine the immunoreactive tissue area, the area of the slide without immunoreactivity was subtracted from the overall area of the field. The microvessel density per tissue section was calculated by determining the average ratio of vessel area to the total tissue in five fields per tissue section.

Vascular Labeling and Drug Diffusion

To assess the functional vasculature, biotin-conjugated *Lycopersicon esculentum* lectin (B1175-1mg, Vector Laboratories) was resuspended in 425 μL PBS and mixed with 75 μL of 1mg/mL Streptavidin-AlexaFluor 633 (S21375, Molecular Probes)(in sterile PBS). Prior to use, the lectin-avidin mixture was centrifuged 14,000k on a microfuge for 10 minutes to remove any particulate. Mice were anesthesized by inhalation of isofluorane gas (2% in oxygen) and placed on a heated platform to minimize the hemodynamic

effects of hypothermia and hypotension that can be caused by infusion of lectins and anesthesia. Fifteen minutes prior to euthanasia, 100 μ l (0.4mg total) of the conjugated lectin was administered as a slow intravenous infusion over 5 minutes, and the hemodynamics monitored closely to ensure that it was tolerated. For doxorubicin experiments, five minutes prior to euthanasia mice were also infused with a 20 mg/kg doxorubicin solution (D-1515.10mg, in sterile saline, Sigma) over one minute.

While under terminal anesthesia, mice were perfused with 4% paraformaldehyde in PBS, pH 7.4. Perfused tissues were harvested, fixed overnight in 4% paraformaldehyde in PBS, pH 7.4 and transferred to 70% ethanol. Tissues were embedded in paraffin, sectioned, rehydrated, and counterstained with DAPI. The lectin labeling experiments were reproduced independently in a second laboratory (SRH, KI).

To evaluate the influence of lectin administration on doxorubicin distribution, 2 KPC mice were infused with doxorubicin only and processed as described above. No differences in the diffusion of doxorubicin were noted. Conversely, several mice (syngeneic, N=2; KPC, N=1) received lectin only to exclude the possibility that doxorubicin interfered with labeling of endothelial cells by *Lycopersicon esculentum* lectin. No differences in lectin labeling were noted in this setting.

Laser Scanning Cytometry

Mice were perfused with 4% paraformaldehyde in PBS, pH 7.4, while under terminal anesthesia. Perfused tissues were harvested, fixed overnight in 4% paraformaldehyde in PBS, pH 7.4 and transferred to 70% ethanol. Tissues were embedded in paraffin,

sectioned, rehydrated, and counterstained with DAPI. Doxorubicin fluorescence was determined by quantitative imaging cytometry using the iCys Research Imaging Cytometer (CompuCyte, Cambridge, MA) with iNovator software (CompuCyte).

A scanning protocol for quantification was configured with two channels. Nuclear DAPI fluorescence was excited by the 405nm diode laser and detected in the blue (445-485nm) channel and doxorubicin fluorescence was excited by the argon 488 nm laser and detected in the orange (565-595nm) channel. The threshold in the DAPI channel was optimised to selectively contour individual cells allowing fluorescence measurement within the primary and peripheral nuclear contours.

High resolution tissue scans were acquired from freshly prepared tissue sections using the 63x objective and 0.5mm step size. Tumour and control areas were defined and doxorubicin fluorescence per cell and cell area measurements were taken from within these regions. Mean tissue autofluorescence was determined in pancreatic tumors and control tissue in four untreated mice, and subtracted from experimental values. Mean fluorescence values and standard deviations for each region were determined as integral fluorescence per cell / cell area.

Immunofluorescence

Mice were infused with 30ml of 4% PFA pH 7.4 using a Harvard Apparatus PhD 2000 syringe pump at a rate of 420ml/min. Tissues were fixed in a 4% PFA pH 7.4 solution for 24 hours and transferred to 70% ethanol. Tissues were paraffin embedded, sectioned and rehydrated. Sections were unmasked in 10mM citric acid in a microwave for 10 minutes. This unmasking procedure was found to effectively quench the fluorescence of

doxorubicin in tissues, allowing the use of additional fluorophores for co-immunofluorescence. Sections were blocked with 10% Serum (Sigma) in TBST and washed in TBST (Tris Buffered Saline; Tween 20, 1%). The following antibody dilutions were used: CD31, 1:75 (sc-1506, Santa Cruz Biotechnology), AlexaFluor 594, 1:1000 (A11059, Invitrogen). Doxorubicin fluorescence was excited with a 488 nm laser, and emission was detected in a range from 520-620nm. Figs. 2B and S2D were imaged using a Nikon CC1Si confocal. All other images were acquired on a Leica SP5 confocal microscope.

Co-immunofluorescence

Tissues were perfused with 4% PFA pH 7.4 solution. Paraffin sections were dewaxed, rehydrated and unmasked in boiling 10mM citric acid pH 6.0. Using the Sequenza Slide staining system (Thermo Scientific Shandon, Cat. 73310017), sections were washed three times in TBST, blocked in 10% serum for 30 minutes, and incubated with both primary antibodies for one hour. Sections were then washed and incubated for 30 minutes secondary fluorophore.

Ki67/Meca32:	Name	Dilution	Company and catalog #
Blocking serum	Goat	10% in TBST	Sigma / G9023
First primary antibody	Rabbit Anti-Ki67	1:500	Thermo Fisher / RM-9106-S1
First secondary antibody	Goat Anti-Rabbit AlexaFluor 488	1:1000	Invitrogen / A11008
Second primary antibody	Rat Anti-Pan ECA (Meca 32)	1:100	Santa Cruz / sc19603
Second secondary antibody	Goat Anti-Rat AlexaFluor 568	1:1000	Invitrogen / A11011

□SMA/Ki67:	Name	Dilution	Company and catalog #
Blocking serum	Goat	10% in TBST	Sigma / G9023
First primary antibody	Rabbit Anti-Alpha Smooth Muscle Actin	1:100	Abcam / ab5694
First secondary antibody	Goat Anti-Rabbit AlexaFluor 488	1:1000	Invitrogen / A11008
Second primary antibody	Rat Anti-Ki67 (Tec3)	1:25	Dako / M7294
Second secondary antibody	Goat Anti-Rat AlexaFluor 568	1:1000	Invitrogen / A11077

For quantification of proliferation in stromal myofibroblasts, five 60X fields of α SMA/Ki67 images were counted from each tumor. Stromal myofibroblasts were identified as α SMA

positive cells that were not associated with blood vessels (pericytes are aSMA positive). For quantification of endothelial proliferation, 10 fields were counted per tumor.

Metastasis Quantification

From each mouse, two lobes of liver were sliced into a total of 6 strips and embedded in paraffin. Microscopic examination of H&E stained sections was used to identify the percentage of mice with at least one metastasis to the liver.

Human Tissues

Histological stains and immunohistochemical assessment of CD31 was performed on archival paraffin patient sections from Addenbrooke's Hospital, and patient specimens from the Johns Hopkins Hospital, in accordance with institutional and national policies at the respective locations.

RNA isolation and quantitative real-time PCR analysis

RNA was isolated from tissues using the RNeasy kit (Qiagen). cDNA was synthesized from 1-2 ug of RNA using the AffinityScript QPCR cDNA Synthesis Kit (Stratagene). cDNA was analyzed by quantitative real-time PCR on a 7900HT Real-Time PCR system using relative quantification ($\Delta\Delta\text{ct}$) with the taqman gene expression assays (Applied Biosystems) shown below. Experiment was performed on 5 KPC tumors and 7 syngeneic tumors derived from K8484 or K8675 cells.

Actin	Mm00607939_s1
dCK	Mm00432794_m1
ENT1	Mm00452176_m1
ENT2	Mm00432817_m1
RRM1	Mm00432794_m1
RRM2	Mm00485881_g1

Gli1	Mm00494645_m1
TK2	Mm00445175_m1

Analysis of VEGF and VEGFR Expression

Whole tumor RNA was extracted from KPC tumors treated for 4 or 8-12 days with vehicle or IPI-926. cRNA was synthesized and hybridized to Illumina Mouse 6 arrays. Expression of VEGF and VEGFR genes was presented as Log₂ relative expression.

Supplementary References

1. F. S. Schreiber *et al.*, *Gastroenterology* 127, 250 (Jul, 2004).
2. M. Niedergethmann *et al.*, *Br J Cancer* 97, 1432 (Nov 19, 2007).
3. K. P. Olive *et al.*, *Cell* 119, 847 (Dec 17, 2004).
4. S. R. Hingorani *et al.*, *Cancer Cell* 7, 469 (May, 2005).
5. N. Cook, K. P. Olive, K. Frese, D. A. Tuveson, *Methods Enzymol* 439, 73 (2008).
6. N. G. Dowell, P. S. Tofts, *Magn Reson Med* 58, 622 (Sep, 2007).
7. P. S. Tofts, A. G. Kermode, *Magn Reson Med* 17, 357 (Feb, 1991).
8. P. S. Tofts, *J Magn Reson Imaging* 7, 91 (Jan-Feb, 1997).
9. M. O. Leach *et al.*, *Br.J Cancer* 92, 1599 (2005).
10. J. L. Abbruzzese *et al.*, *J Clin Oncol* 9, 491 (Mar, 1991).

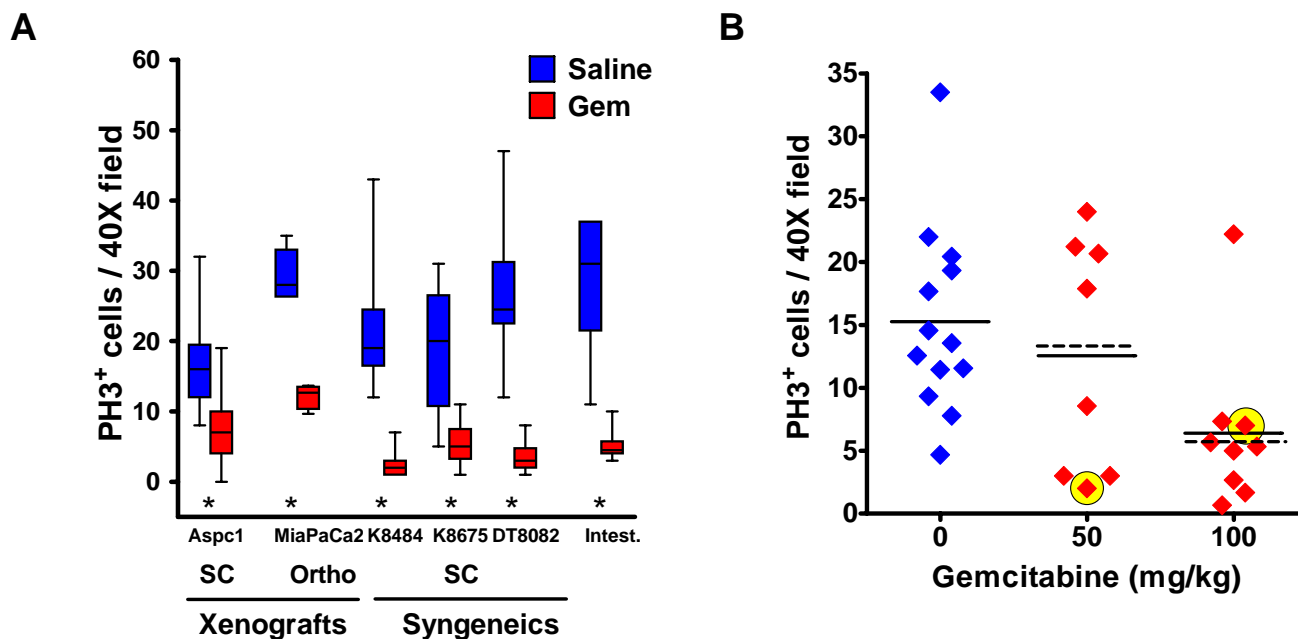


Figure S1. Figure 1. KPC pancreatic tumors are predominantly resistant to gemcitabine. Murine pancreatic tumor models were challenged with saline (blue) or gemcitabine (red), Q3Dx4. A final dose of gemcitabine was administered four hours prior to euthanasia. * $P < .05$, Mann-Whitney U. Solid lines = mean; dashed lines = mean without responders. **(A)** Immunohistochemistry for phospho-histone H3 (PH3) was quantified, revealing significantly fewer cells in mitosis in gemcitabine-treated transplanted tumors. Positive control: small intestine. **(B)** Phospho-histone H3 staining was significantly diminished in KPC tumors treated with 100mg/kg gemcitabine ($P = .003$, Mann-Whitney U), but to a lesser extent than in transplanted tumors.

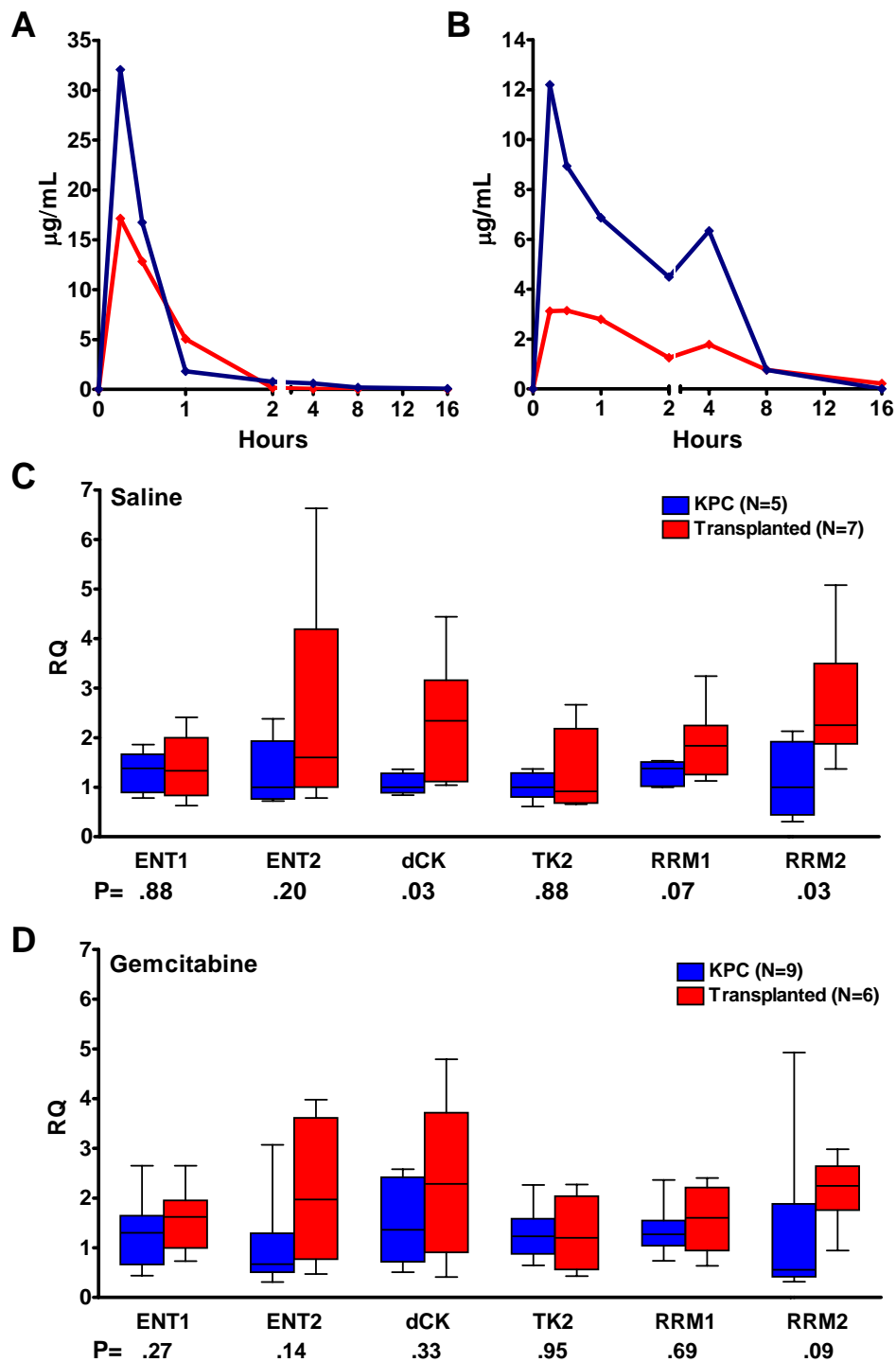


Figure S2. Gemcitabine metabolism does not explain the distinct responses of KPC and transplanted tumors. Wild-type mice were treated with a single 100mg/kg dose of gemcitabine at various timepoints. Plasma was collected and analyzed for gemcitabine (dFdC) (A) and its inactive metabolite, dFdU (B), by HPLC. Lines indicate average data for two males (red) and two females (blue). Gemcitabine was rapidly metabolized in murine plasma, correlating with an accumulation of dFdU. (C) Quantitative RT-PCR was performed on RNA from transplanted (red) or KPC (blue) tumors for genes implicated in the cellular response to gemcitabine: equilibrative nucleotide transporters 1 and 2 (ENT1, ENT2), deoxycytidine kinase (dCK), thymidine kinase 2 (TK2) and ribonucleotide reductase subunits 1 and 2 (RRM1, RRM2). P-values for Mann-Whitney U tests are indicated below each gene, showing significant differences only in dCK and RRM2 (C). These differences were less apparent in cohorts of tumors treated for 12 days with 100mg/kg gemcitabine, Q3Dx4. (D).

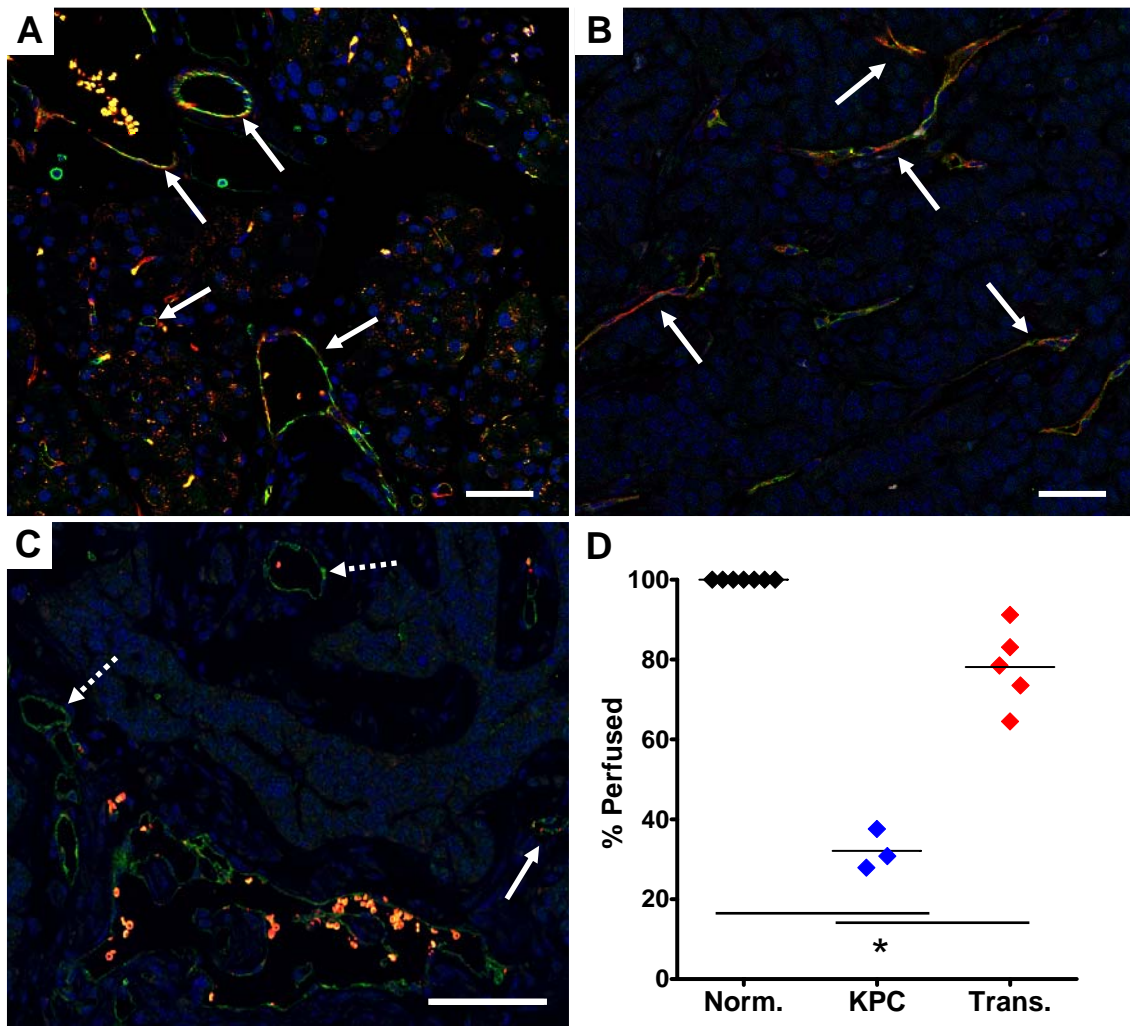


Figure S3. Vessel patency is compromised in KPC tumors. In order to visualize the fraction of perfused blood vessels, Alexafluor 633-labelled *L. esculentum* lectin (red) was infused 15 minutes prior to euthanasia and visualized in combination with CD31 immunofluorescence (green). Perfused vessels exhibited both red and green labeling (arrows), while non-perfused vessels appear green (dotted arrows). **(A)** In normal pancreas tissues, all blood vessels were perfused. **(B)** In transplanted tumors, most vessels were perfused. **(C)** In KPC tumors, most vessels were not perfused. **(D)** The percent of CD31+ vessels that were also marked with lectin was quantified for normal pancreas, transplanted and KPC tumors. Significantly fewer blood vessels in KPC tumors were perfused than in transplanted tumors or normal pancreas ($P < .04$, Mann-Whitney U). Scale bars = 100uM.

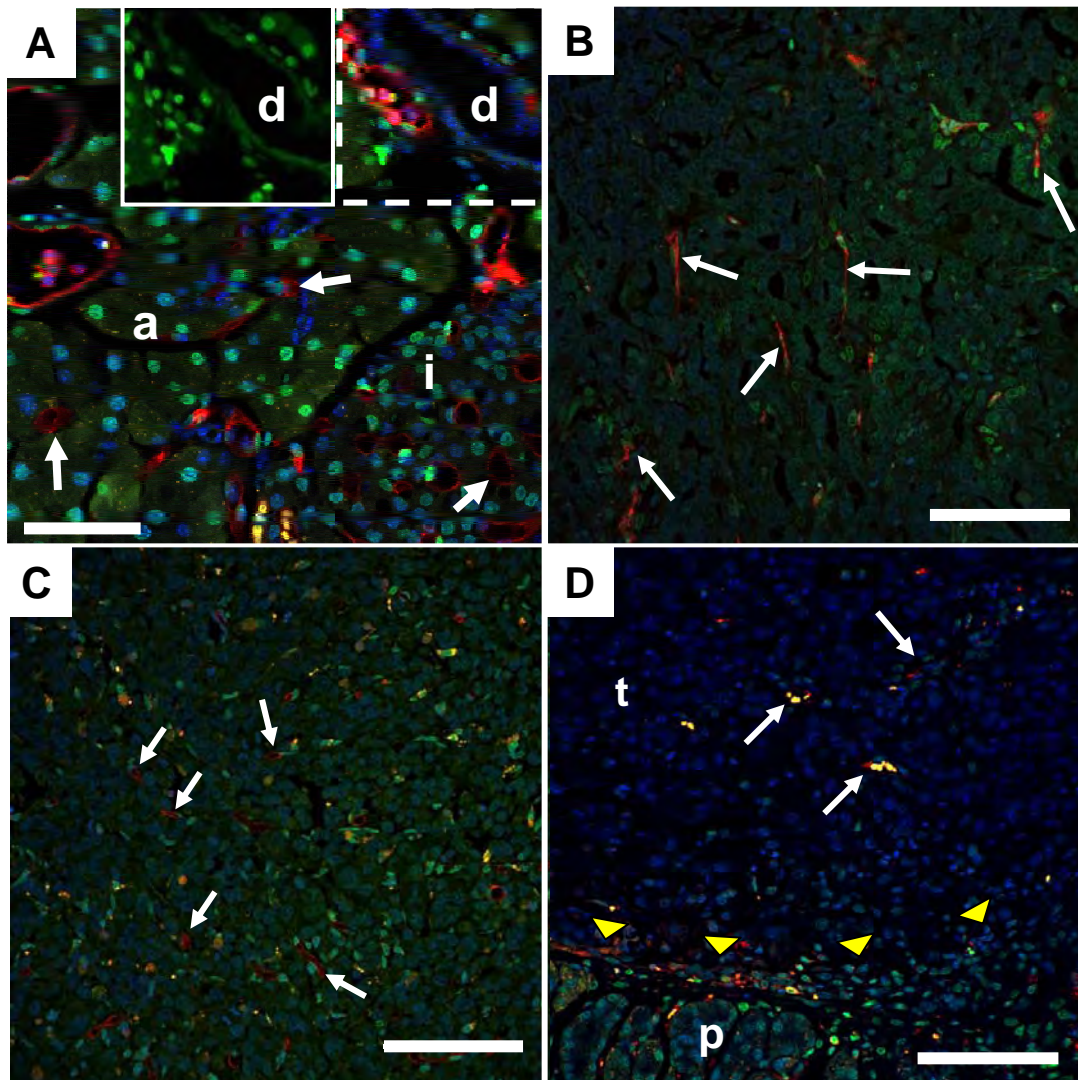


Figure S4. KPC tumors are poorly perfused. In order to visualize the delivery and diffusion of a small molecule, lectin (red) was infused as in Figure S3 and, additionally, doxorubicin (green) was infused 5 minutes prior to euthanasia. Paraffin sections were stained with DAPI (blue) and visualized by direct immunofluorescence. Doxorubicin is effectively delivered to normal tissues (**A**)(N=5), subcutaneous transplanted tumors (**B**)(N=5) and orthotopic transplanted tumors (**C**)(N=2). In panel (**A**), a = acinar, i = Islets, d = ducts, and left inset panel shows only the doxorubicin channel, demonstrating doxorubicin uptake in normal ductal cells. (**D**) In contrast, few perfused vessels and very little doxorubicin staining is apparent in the invasive area (t) of KPC tumors (N=3). Doxorubicin perfusion is apparent in surrounding pancreatic tissue (p) and immediately adjacent to the few lectin-labeled vessels present in the tumor (arrows). Yellow triangles denote the sharp demarcation between tumor and adjacent acinar pancreatic tissue. Scale bars, panel (**A**) = 50uM, panels (**B-D**) = 100uM.

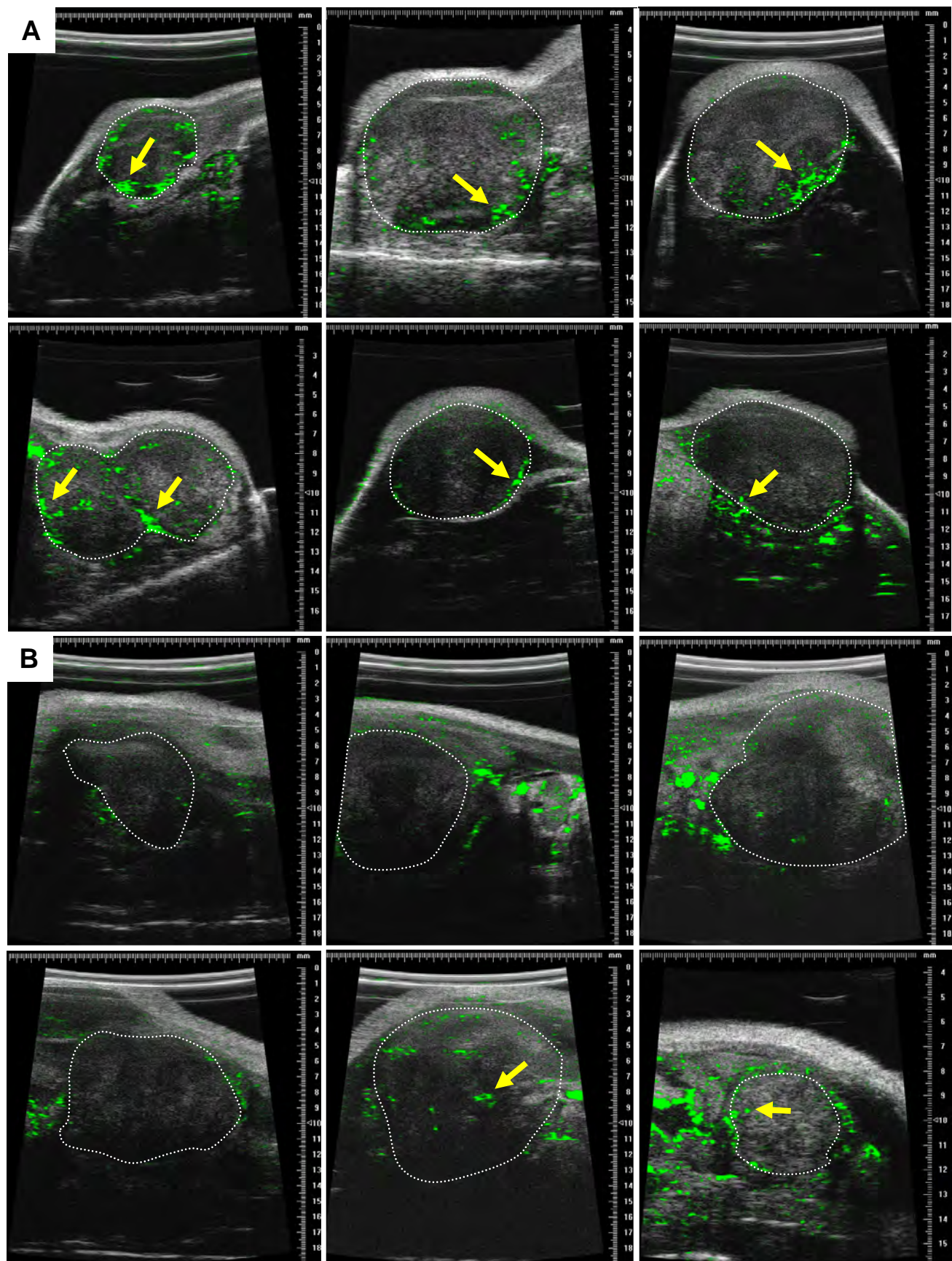


Figure S5. KPC pancreatic tumors are poorly perfused. High resolution contrast ultrasound was used to visualize the delivery of $5\mu\text{M}$ gas-filled liposomes (green) to transplanted (A) and KPC (B) tumors. Dotted lines indicate borders of tumor based on anatomical ultrasound. Arrows denote well-perfused areas of tumor parenchyma. Transplanted tumors were rapidly perfused in their periphery, particularly along their basolateral surfaces. In contrast, most KPC tumors were poorly perfused within the tumor parenchyma, despite adequate perfusion of surrounding tissues. Scales in millimeters.

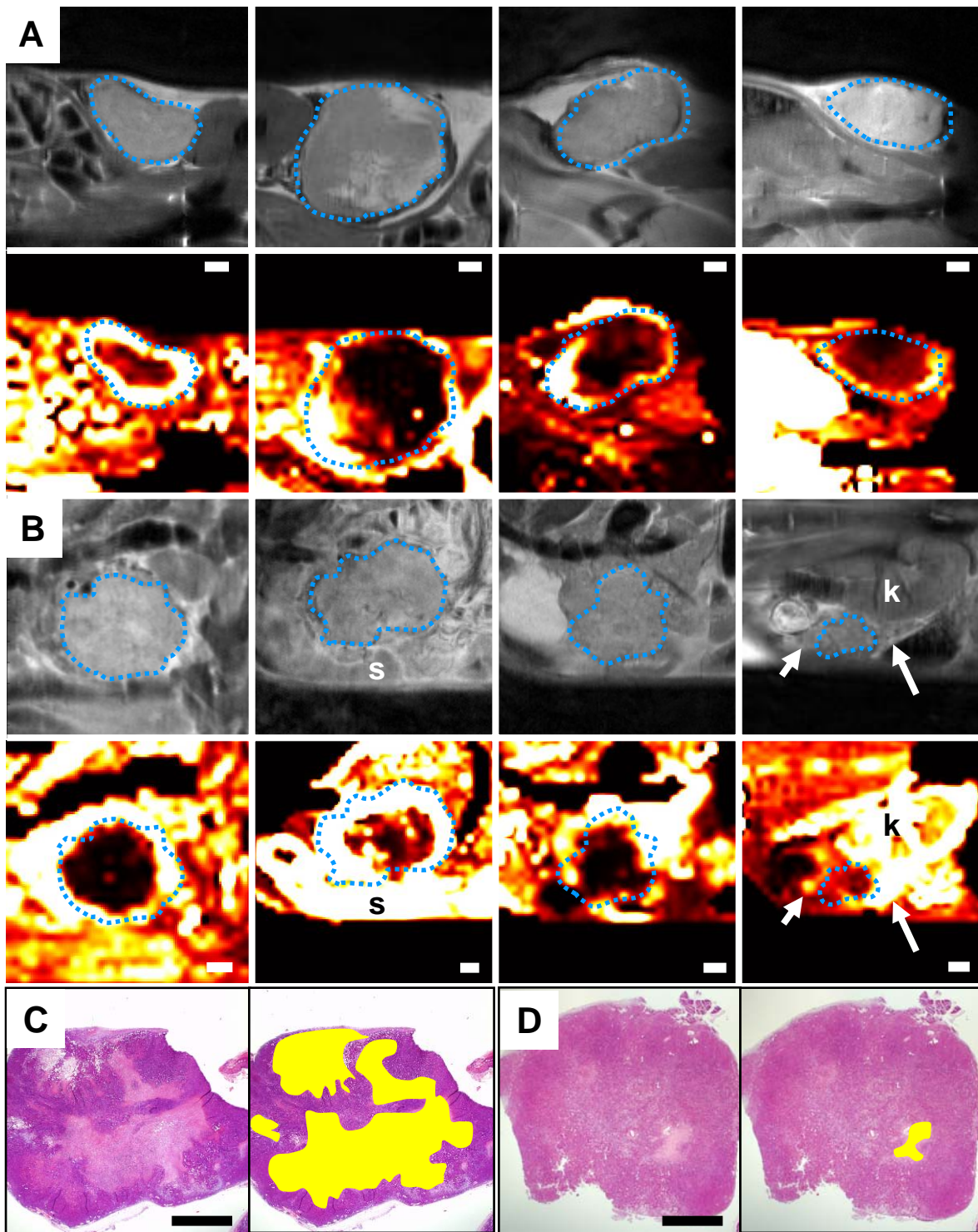


Figure S6. Perfusion and extravasation of Gd-DTPA is compromised in KPC pancreatic tumors. The MRI contrast agent Gd-DTPA was administered to anaesthetized mice and uptake by transplanted (A) and KPC (B) tumors was measured by DCE-MRI. Ktrans values (a value that incorporates both the perfusion and extravasation of Gd-DTPA) were mapped onto T2-weighted anatomical images (grayscale), with high values indicating effective delivery/retention (white/yellow) and low values indicating poor delivery/retention (red/black). Tumor outlines denoted by blue dotted lines. Scale bars = 2mm, s = spleen, k = kidney, arrows indicate adjacent normal pancreas. Strong enhancement was observed in the peripheral regions of transplanted tumors, corresponding to the viable regions of tumor parenchyma. In contrast, poor enhancement was observed in most KPC tumors, despite significant enhancement of adjacent tissues and low levels of necrosis. Example H&E sections of transplanted (C) and KPC (D) tumors, with necrotic areas indicated yellow in duplicate panels.

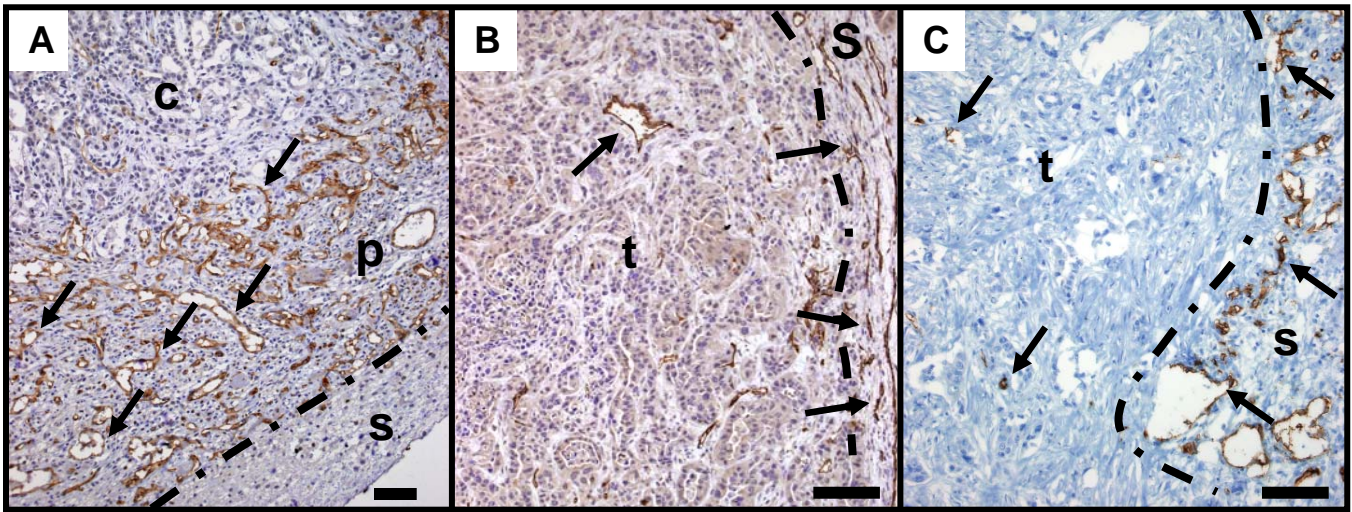


Figure S7. KPC pancreatic tumors are poorly vascularized. CD31 immunohistochemistry was performed on transplanted (A) and KPC (B) tumors as well as human pancreatic ductal adenocarcinomas (C). Scale bars = 50µM. Arrows denote blood vessels. Hashed lines denotes border between tumors and surrounding tissues. Peripheral regions of transplanted tumors (p) were densely vascularized compared to surrounding tissues (s) and more central regions (c). In contrast, few blood vessels were apparent in the parenchyma of KPC and human tumors (t) despite extensive vascularization of surrounding tissues (s).

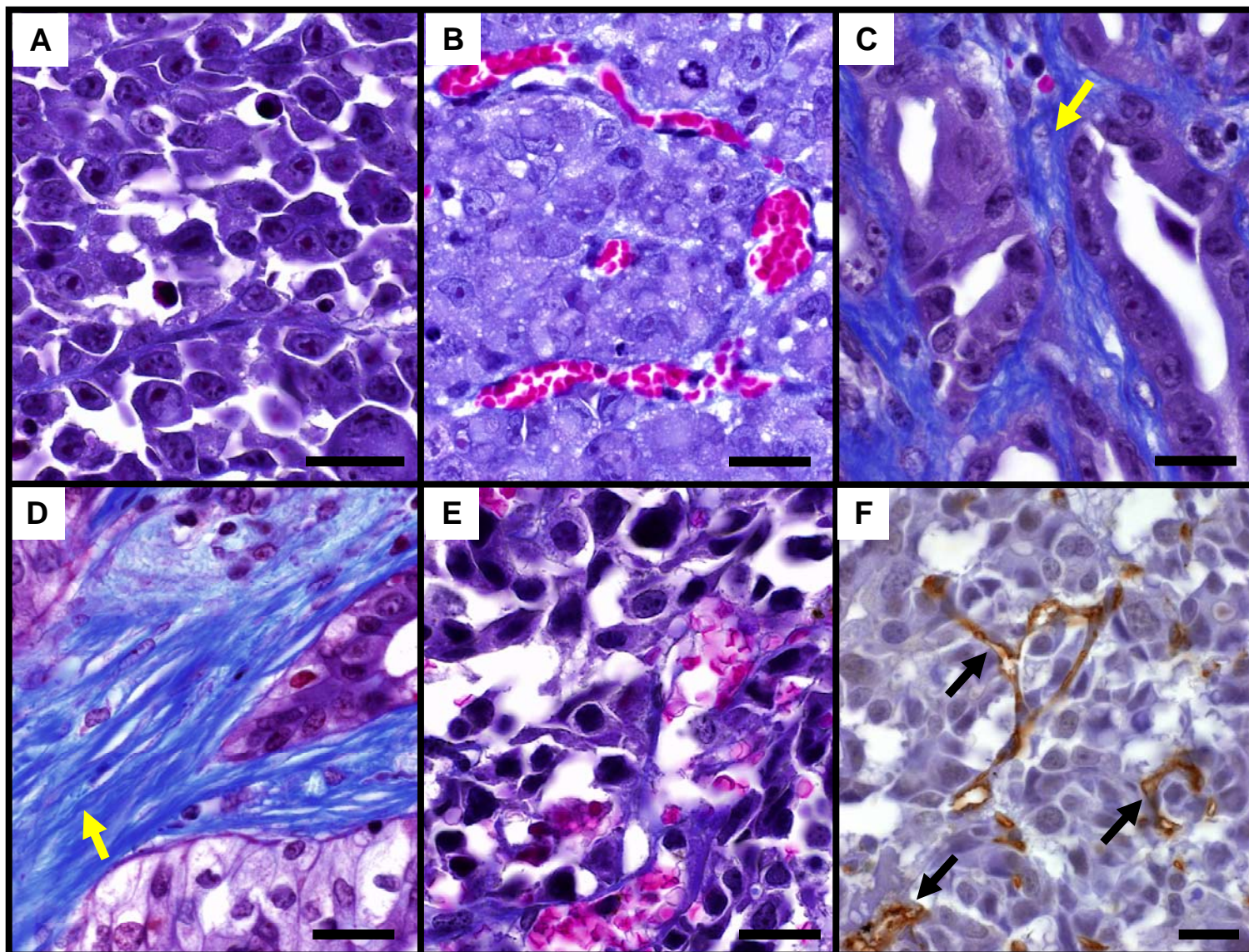


Figure S8. KPC pancreatic tumors have a distinct stromal architecture. Masson's trichrome was used to visualize the extracellular matrix (blue) of syngeneic (A) and orthotopic (B) transplanted tumors, as well as KPC tumors (C) and primary human pancreatic tumors (D). Yellow arrows indicate stromal fibers. Transplanted tumors are typically stroma-poor while KPC and human pancreatic tumors have a prominent desmoplastic stroma. Of note, the two gemcitabine-sensitive tumors (E) had a lower stromal content than other KPC tumors. (F) This correlated with a dense vasculature, as visualized by CD31 IHC. Black arrows indicate blood vessels. Scale bars = 20µm.

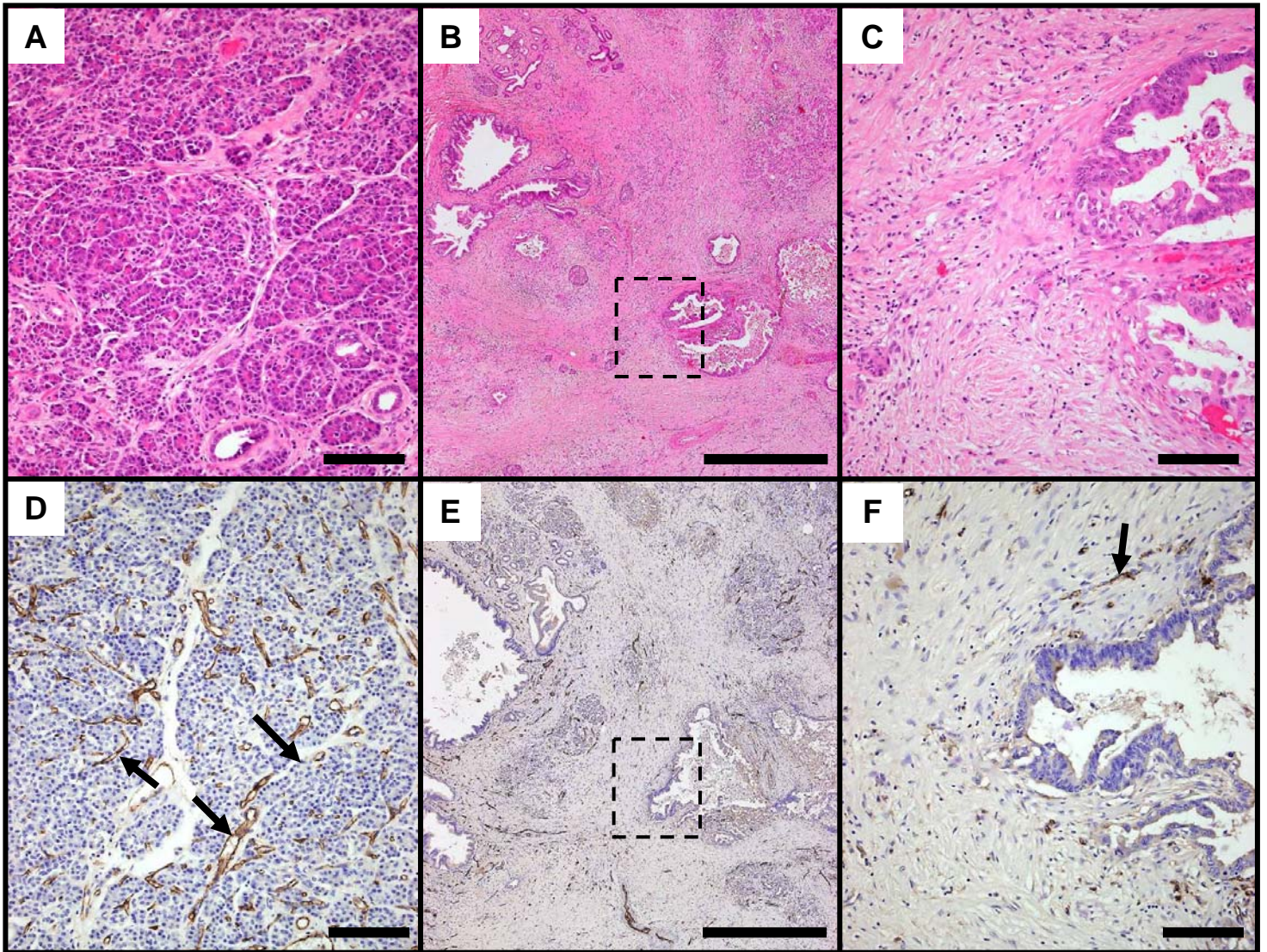


Figure S9. Human pancreatic tumors are hypovascular. Human pancreas (**A,D**) or pancreatic ductal adenocarcinomas (**B,C,E,F**) were stained with H&E (**A-C**) and adjacent sections were immunostained for CD31 (**D-F**). Dashed boxes in (**B**) and (**E**) indicate regions shown at higher magnification in (**C**) and (**F**), respectively. Similar to observations in KPC mice, human normal pancreatic tissue contains a dense network of fine capillaries surrounding the acini and ducts (arrows), whereas regions of invasive cancer exhibit significantly fewer blood vessels. Scale bars in panels (**A,D,C,F**) = 50 μ m; scale bars in panels (**B,E**) = 200 μ m.

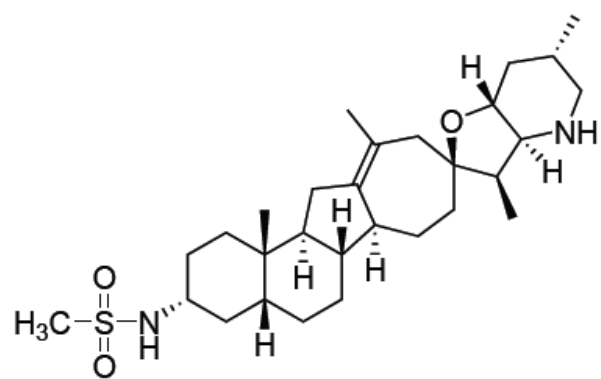


Figure S10. Chemical structure of IPI-926.

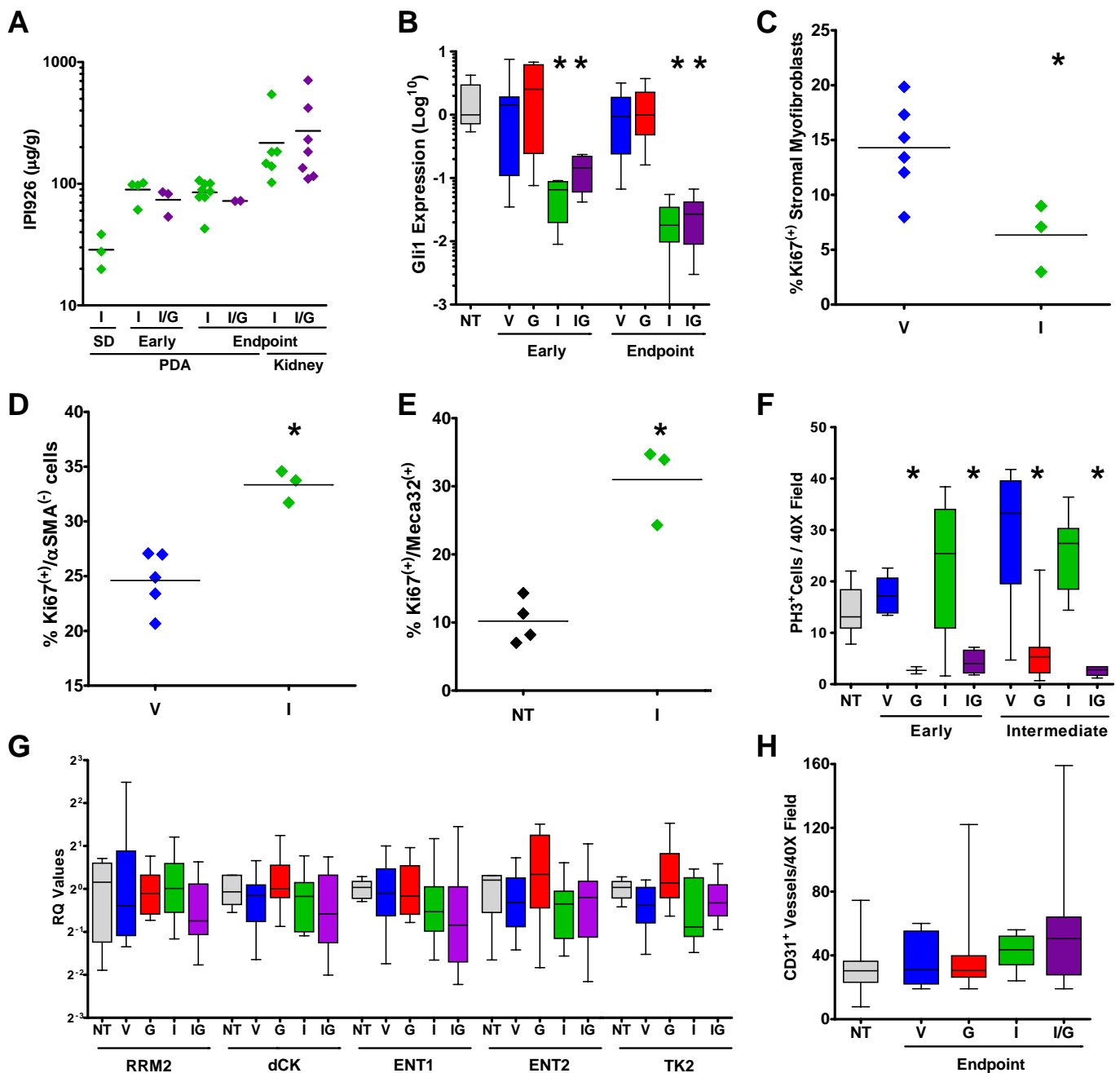
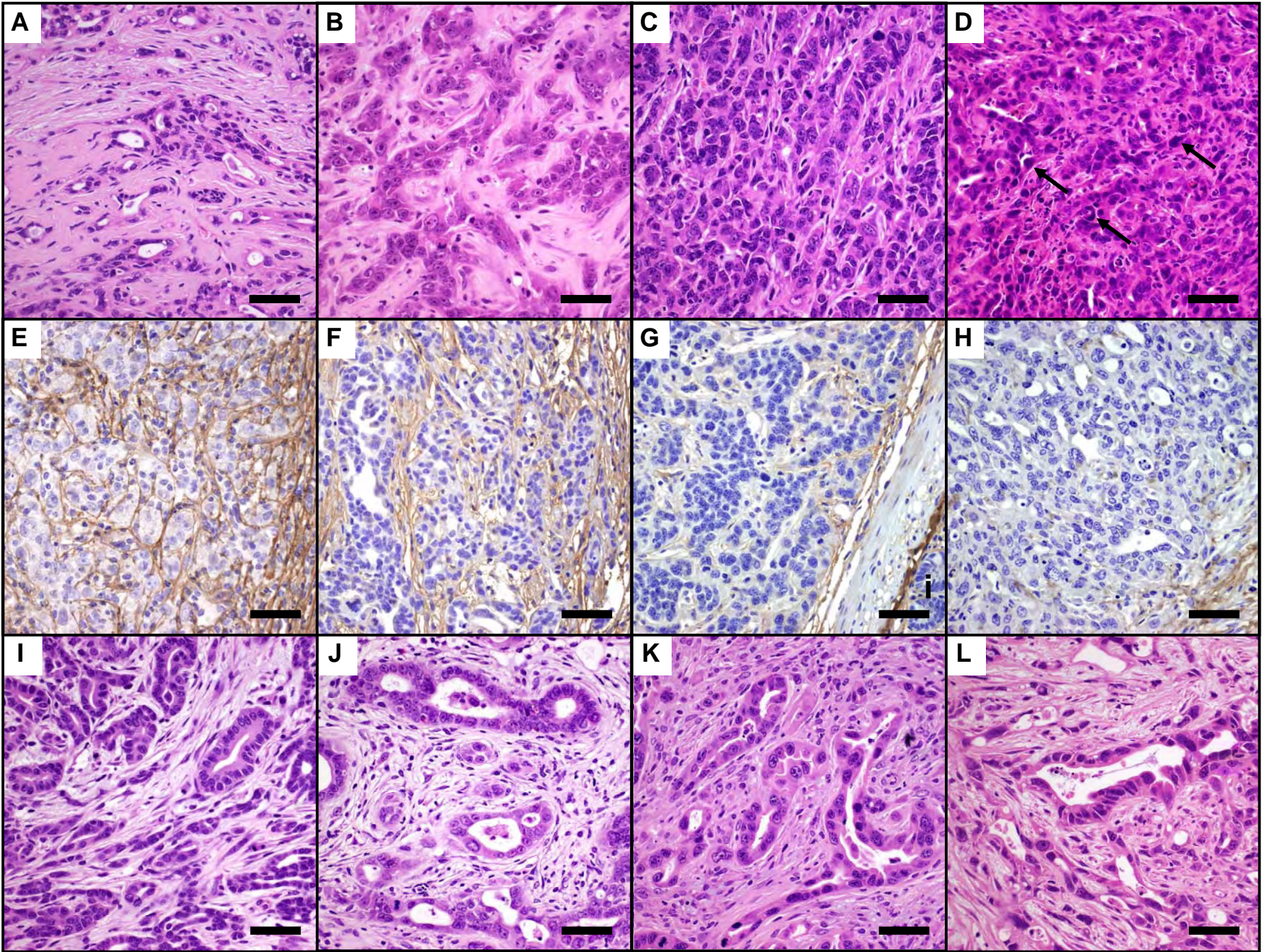


Figure S11. Treatment of KPC tumors with IPI-926 promotes drug delivery. (A) Levels of IPI-926 were determined in extracted tumor or kidney tissues from KPC mice treated with a single dose of IPI-926 (SD), daily for four days (Early), or as part of a survival study (Endpoint). IG indicates mice also treated with gemcitabine. IPI-926 accumulated in tumor tissues over the course of four days, but remained significantly lower than in kidney tissues. (B) Real-time PCR analysis found that Gli1 levels were significantly reduced in KPC tumors after four days of IPI-926 treatment and at endpoint ($*P < .003$, Mann-Whitney U) and were unaffected by treatment with gemcitabine. (C) Coimmunofluorescence for the fibroblast marker α SMA and the proliferation marker Ki-67 was performed on KPC tumors treated with vehicle or IPI-926 for four days. The percentage of stroma myfibroblasts that were Ki67 positive was scored. As α SMA marks pericytes in addition to fibroblasts, lumen-forming α SMA positive cells were excluded from analysis. The proliferation rate of stromal myfibroblasts was significantly lower in IPI-926 treated tumors ($*P < 0.03$, Mann-Whitney U). (D) In the previous experiment, the proliferation rate of α SMA negative cells was significantly increased in IPI-926 treated tumors ($*P < .05$, Mann-Whitney U). (E) Coimmunofluorescence for the endothelial marker Meca32 and the proliferation marker Ki-67 was performed on tumors treated with vehicle or IPI-926 for 10 days. Endothelial cell proliferation was significantly increased in IPI-926 treated tumors ($*P < .05$, Student's T). (F) The frequency of mitotic cells in KPC tumors (determined as in Fig. 1) was decreased after 4 days (early) or 8-12 days (intermediate) of treatment with gemcitabine or IPI-926/gem, but was unaltered in tumors treated only with IPI-926. (G) The expression of genes implicated in gemcitabine chemoresistance was determined by real-time RTPCR, as in figure S2, on KPC tumors from the survival study. No significant differences were found between treatment groups. (H) MVD was determined as in Figure 3D for KPC tumors from the survival study. The vessel density of IPI-926 and IPI-926/gem treated tumors was significantly lower at endpoint than after 8-12 days (compare to Figure 3D, $P < .05$, Mann-Whitney U).



Olive et. al, Figure S12

Figure S12. Histopathology of KPC tumors treated with IPI-926. KPC tumors were treated for 8-12 days (**A-H**) or 4 days (**I-L**) with vehicle (**A,E,I**), gemcitabine (**B,F,J**), IPI-926 (**C,G,K**) or IPI-926/gem (**D,H,L**). Scale bars = 100µm. (**A-D**) H&E stained sections demonstrate the loss of cellular and acellular stroma following treatment with IPI-926 and IPI-926/gem, resulting in densely packed tumor cells. The histopathology of IPI-926/gem treated tumors was highly heterogeneous, including anaplastic regions of extreme nuclear and cellular atypia (arrows). (**E-H**) Collagen I IHC demonstrates the loss of extracellular matrix fibers in IPI-926 treated tumors. The right side of each panel is located near the periphery of each tumor to show positive staining. i = adjacent intestine tissue in panel (**G**). (**I-L**) H&E stained sections demonstrate that desmoplastic stroma is still present in IPI-926 treated tumors after 4 days of treatment.

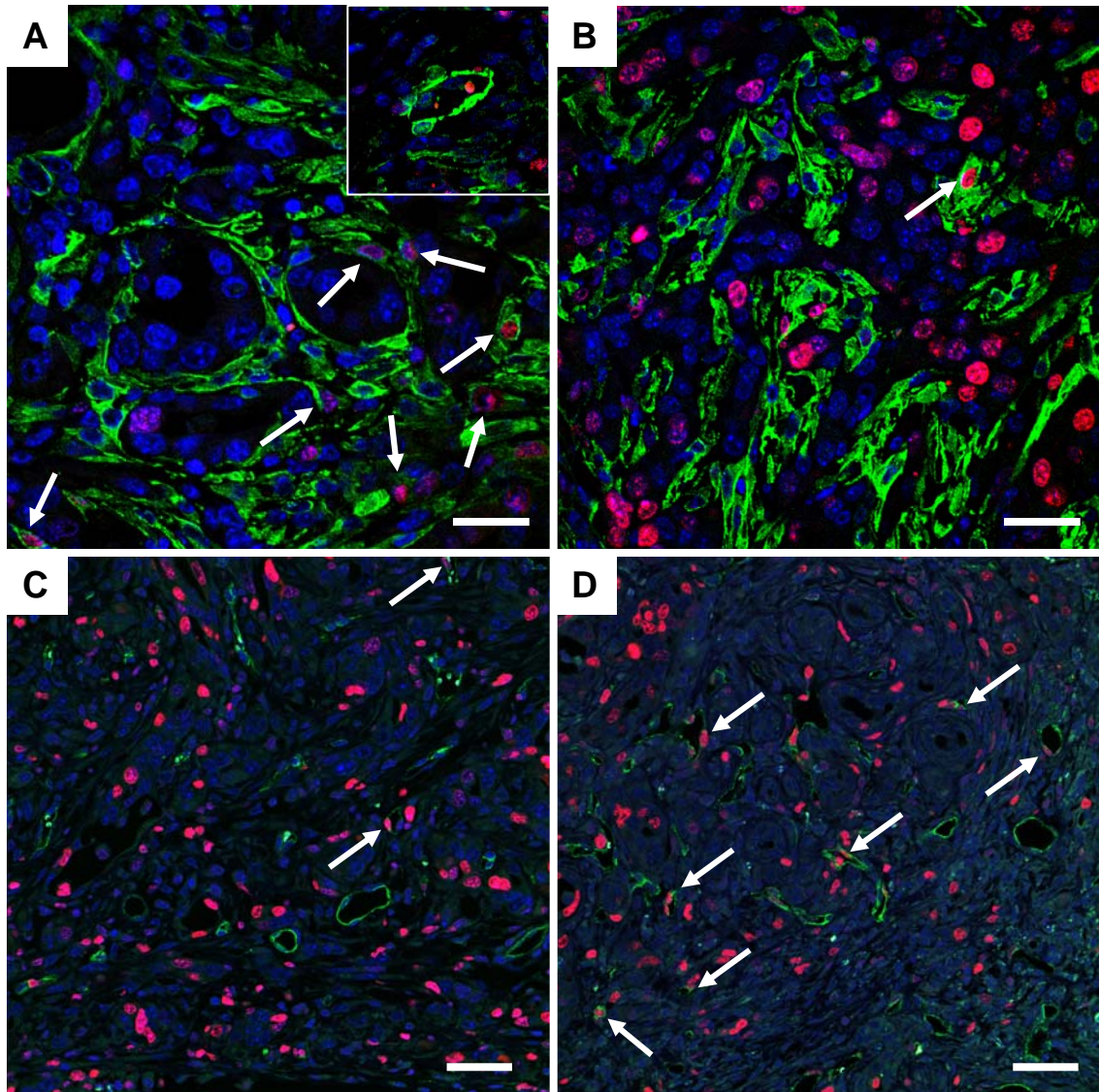
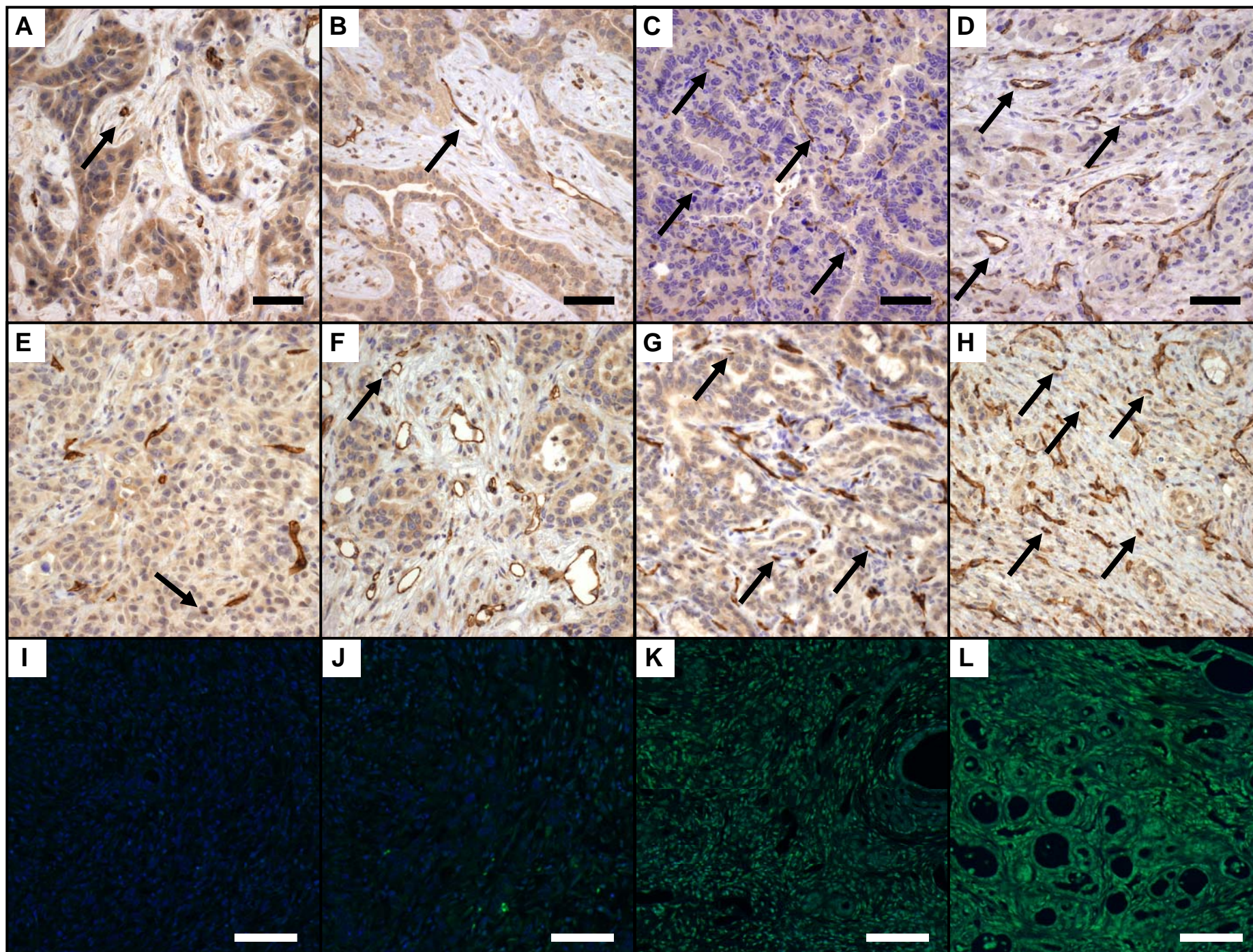


Figure S13. IPI-926 treatment increases endothelial proliferation and decreases fibroblast proliferation. Coimmunofluorescence for the fibroblast marker α SMA (green) and the proliferation marker Ki-67 (red) was performed on KPC tumors treated for four days with vehicle (**A**) or IPI-926 (**B**). Arrows indicate examples of α SMA/Ki-67 double positive cells. Pericytes, identified as lumen-forming α SMA positive cells (inset), were excluded from analysis. Coimmunofluorescence for the endothelial marker Meca32 and the proliferation marker Ki-67 was performed on tumors treated for 10 days with vehicle (**C**) or IPI-926 (**D**). Arrows indicate examples of proliferating endothelial cells (Meca32+/Ki-67+). Scale bars in (**A,B**) = 50 μ M, in (**C,D**) = 100 μ M.



Olive et. al, Figure S14

Figure S14. IPI-926 increases vascularization and drug delivery in KPC tumors. KPC tumors were treated for 8-12 days (**A-D, I-L**) or 4 days (**E-H**) with vehicle (**A,E,I**), gemcitabine (**B,F,J**), IPI-926 (**C,G,K**) or IPI-926/gem (**D,H,L**). Scale bars = 100 μ m. (**A-D**) CD31 IHC demonstrates increased vessel density in IPI-926 treated tumors after 8-12 days. (**E-H**) This trend is apparent after only 4 days of treatment. At this early timepoint, numerous isolated CD31 positive cells (arrows) are apparent in IPI-926 treated tumors. (**I-L**) After 8-12 days of treatment, mice were administered doxorubicin 5 minutes prior to euthanasia and doxorubicin autofluorescence (green) was imaged. Blue = DAPI. Increased levels of doxorubicin were detected in IPI-926 treated tumors.

Figure S15. KPC tumors respond transiently to IPI-926/gem treatment. Two growth curves are presented for KPC mouse in the survival study. On the left, tumor volume over the first 10 days of treatment is shown, normalized to the tumor volume at the start of treatment, with a variable Y-axis. On the right, the entire growth curve for each mouse is presented using identical X- and Y-axes.

HPLC	ID	Dose (mg/kg)	PDA or Pancreas		Spleen	
			dFdCTP (nmol)	ATP (nmol)	dFdCTP (nmol)	ATP (nmol)
Pancreas	K9548	100	0.058	0.443	0.365	2.087
	K9788	100	BLQ	0.538	0.103	1.503
	K9487	50	0.356	0.638	0.078	0.682
KPC	K9052	100	BLQ	1.334	0.049	4.373
	K9559	100	BLQ	0.937	0.101	2.742
	K9354	100	BLQ	0.483	ND	ND
	K9771	50	BLQ	0.749	BLQ	0.34
Transplanted	AG12C	100	0.148	1.4	ND	ND
	AG13D	100	0.044	1.816	ND	ND
	AG10D	100	0.035	1.631	ND	ND
	AG10C	100	0.044	2.283	ND	ND
	XG21B	100	BLQ	0.284	0.143	5.072
	XG22B	100	BLQ	2.29	0.079	4.441
	XG21A	100	0.041	0.473	0.143	5.072
	XG22A	100	0.153	4.448	0.079	4.441
	XG31A	100	0.133	5.371	0.036	2.473
	XG32A	100	0.026	0.787	0.17	3.522

Table S1. Pharmacokinetic analyses. dFdCTP and ATP were detected by HPLC in spleen, normal pancreas or tumor tissue from KPC or transplanted tumor models . Suitability of the tissue was determined by the level of ATP in the sample. BLQ = below limit if quantification.

A.

	4 Days				
	Vehicle	SE	IPI-926	(SE)	P-value
vegf-a	0	0.912	0.290	1.457	0.739
vegf-b	0	0.260	-0.045	0.208	0.769
vegf-c	0	0.548	0.284	0.278	0.304
flt1	0	0.061	0.004	0.072	0.927
flt4	0	0.017	-0.017	0.032	0.373
kdr	0	0.036	0.012	0.030	0.568

B.

	8-12 Days				
	Vehicle	SE	IPI-926	(SE)	P-value
vegf-a	0	0.553	0.340	0.370	0.263
vegf-b	0	0.464	0.117	0.557	0.717
vegf-c	0	0.493	0.040	0.360	0.879
flt1	0	0.075	-0.002	0.033	0.962
flt4	0	0.068	0.009	0.038	0.794
kdr	0	0.029	-0.011	0.040	0.609

Table S2. Expression of vegf genes in KPC tumors treated with IPI-926. KPC mice were treated for 4 days (A) or 8-12 days (B) with vehicle or IPI-926. Gene expression array analysis was performed on mRNA extracted from tumor tissue samples. Results are normalized to mean of vehicle-treated groups and shows Log₂ relative expression.